# We are IntechOpen, the world's leading publisher of Open Access books Built by scientists, for scientists

6,900
Open access books available

185,000
International authors and editors

200M
Downloads

Our authors are among the

154
Countries delivered to

TOP 1%
most cited scientists

12.2%
Contributors from top 500 universities




WEB OF SCIENCE™

Selection of our books indexed in the Book Citation Index in Web of Science™ Core Collection (BKCI)

## Interested in publishing with us?
## Contact book.department@intechopen.com

Numbers displayed above are based on latest data collected.
For more information visit www.intechopen.com



Chapter 2

# Temporal Variation of Particle Size Distribution of Polycyclic Aromatic Hydrocarbons at Different Roadside Air Environments in Bangkok, Thailand

Tomomi Hoshiko, Kazuo Yamamoto,
Fumiyuki Nakajima and Tassanee Prueksasit

Additional information is available at the end of the chapter

http://dx.doi.org/10.5772/48432

## 1. Introduction

Polycyclic aromatic hydrocarbons (PAHs) have been drawing attention as a major hazardous air pollutant due to their potential carcinogenicity and mutagenicity [1-2]. Polycyclic aromatic hydrocarbons are formed during the incomplete combustion of oil, coal, gas, wood and other organic substances. PAHs are initially generated in the gas phase, and they are adsorbed on pre-existing particles undergoing condensation during further cooling of the emission. Thus, most atmospheric PAHs exist in the particulate phase, while some higher volatility PAHs or low molecular weight PAHs remain partly in the gas phase (e.g., [3]). There are basically five major emission source components: domestic, mobile, industrial, agricultural and natural. The relative importance of these sources changes depending on the place or regulatory views; however, in the urban environment with heavy traffic, mobile source, that is vehicle exhaust is the main contributor to the atmospheric PAHs (e.g., [3-6]). Thus, health risk of the dense urban population by the exposure to those PAHs has been of concern both in developed and developing countries.

Currently, PM10 or finer particles are major air pollutants in many urban areas. In the atmosphere, PAHs are partitioned between gaseous and particulate phases as explained earlier. Especially, PAHs of higher molecular weight species, which are often of higher carcinogenic potential, are mostly associated with fine particulate matter (e.g., [2, 7]). However, atmospheric behavior of particulate matter is known to be highly complicated in terms of its chemical compositions, size distributions, physical behavior, reactions, and so on. Accordingly, atmospheric behavior of PAHs associated with particulate matter is subjected to uncertainties and still poorly explained, including their temporal and spatial variations.

INTECH
open science | open minds

© 2012 Hoshiko et al., licensee InTech. This is an open access chapter distributed under the terms of the Creative Commons Attribution License (http://creativecommons.org/licenses/by/3.0), which permits unrestricted use, distribution, and reproduction in any medium, provided the original work is properly cited.

Thailand's capital city, Bangkok was selected as the field of this study, where traffic air pollution and its health effects have long been a serious problem due to the heavy traffic and the chronic state of traffic congestion. It was reported that about 88% of PAH emission is attributed to motor vehicles, and a minor contributions are from biomass burning and oil combustion [6]. In Bangkok, road traffic is the main transport. Diesel buses have been the primary public transport, and ownership of passenger cars- both gasoline and diesel- and motorcycles has been increasing. The mass rapid transit network is still insufficient to meet the dramatically increased travel demand, which arose concurrently with the rapid economic development and rise in population in the last several decades. Thus, road traffic is heavily congested. At present, overall air quality in Bangkok has been significantly improved owing to several effective policies taken in the last decade, and the initiation and ongoing extension of railways and reinforcement of vehicle emission controls are quite promising for the further improvement. This is recognized as a successful case of urban air quality improvement in Southeast Asia, where many cities are still suffering from serious air pollution. In spite of the improvement, the present roadside PM10 levels in Bangkok have still been constantly exceeding the standard values; 24 hour standard 120 $\mu g/m^3$ and annual standard 50$\mu g/m^3$ [8]. Given the situation, carcinogenic PAHs associated with particulate matter are suspected to contribute to an increased health risk for the people living in the city.

Previous studies on roadside measurements reported much higher levels of PAHs than those at ambient sites, which has been the case for Bangkok as well [6,9-13]. It is stressed that environmental monitoring of PAHs is needed in more comprehensive ways with higher resolutions of time and space, especially at roadside areas, which are possible hot spots of high levels of exposure. In PAH monitoring, temporal variations of concentrations are an important aspect, for example, seasonal and diurnal changes. As for seasonal variations, monitoring data in developed countries in the temperate regions, such as Western Europe and the USA, are relatively abundant, whereas in developing countries in the tropical regions including Thailand, data are limited. For diurnal variations, there have not been many cases reported because PAH concentrations are usually reported as daily average. However, some previous reports showed remarkable diurnal changes in PAH concentrations, with morning and evening peaks in parallel with traffic rush hours (e.g., [5,12,14-17]). If we further look into the behavior of PAHs, information on diurnal variations of particle size-fractioned PAH concentrations become of interest, because particulate matter of different sizes is known to exert different levels of adverse health effects in the human body and finer particles penetrate into deeper parts of the human body and cause respiratory or cardiovascular disorders. However, studies concerning such information have been quite limited. Therefore, the specific objective of this study is to investigate diurnal variations of particle size distribution of PAHs by conducting field measurements.

## 2. Methodology

### 2.1. Study sites and time

Bangkok has a population of more than eight million people. Its climate is classified as tropical savanna with three seasons: hot (March – mid May), wet (mid-May - October) and

cool (November - February). In terms of their characteristics, the hot season is hot and dry, the wet season is hot and wet, and the cool season is cool and dry. Field measurements were conducted in March and April, 2006, in the hot season. Concentrations of particulate phase PAHs were measured on the roadside in Bangkok. Diurnal variations of PAH concentrations were investigated by comparing two roadside sites with different road configurations. The measurement sites were Rama6 (R6) and Chockchai4 (CC). The R6 site is located in the area of government offices in the Bangkok city center, where one of the main roads, R6, carries heavy traffic. The R6 road is covered by an elevated highway (Figure 1a), and this configuration, together with large roadside buildings, is likely to cause a stagnant air mass within the road space. By contrast, the CC site has an ordinary open-space configuration along the Ladphrao road, with low-rise small buildings (Figure 1b). The measurement points were approximately three meters distance from the roads at both sites, 1.5 meters height from the ground at R6 (Figure 2a) and three meters height at CC in a Pollution Control Department's (PCD) air monitoring station, where the rooftop space of the station was provided to install measurement equipment for this study (Figure 2b).



(a) (b)

**Figure 1.** Figure 1. Study sites. a) Rama6; b) Chockchai4

## 2.2. Air sampling

Particle mass was collected using a 10-stage Micro Orifice Uniform Deposit Impactor (MOUDI, Model 110, MSP Corporation, U.S.A.) [18] (Figure 3). The principle operation of the MOUDI is the same as any inertial cascade impactor with multiple nozzles. At each stage, jets of particle-laden air impinge upon an impaction plate, and particles larger than the cut-size of that stage cross the air stream lines and are collected upon the impaction plate. The smaller particles with less inertia do not cross the streamline and proceed to the next stage where the nozzles are smaller and where the air velocity through the nozzle is higher, and there, the finer particles are collected. This continues through the cascade impactor until the smallest particles are collected by the after-filter [19]. Figure 4 shows a schematic diagram of one stage of the MOUDI, showing its relation to the above and below stages [19].



(a) (b)

**Figure 2.** Measurement locations. a) Rama6; b) Chockchai4



**Figure 3.** Micro Orifice Uniform Deposit Impactors (MOUDI)

Polytetrafluoroethylene (PTFE) membrane filters of 47-mm diameters (ADVANTEC, Japan) were used as the impaction substrates, and 37-mm glass filters (ADVANTEC, Japan) were used as the after-filter. The aerodynamic diameter size cut points with 50% collection efficiency were 0.18, 0.31, 0.56, 1.0, 1.8, 3.2, 5.6, 10, and 18 μm. The MOUDI operated at 30 L/min, and the particle mass in the filters was determined gravimetrically. Before each weighing, the filters were conditioned in a desiccator with silica gel for about three days to eliminate humidity. Afterward, the filters were wrapped in aluminum foil and stored at 4 °C until the extraction was performed. After ultrasonic extraction, 13 kinds of PAHs with three to six aromatic rings (Table 1 and Figure 4) were determined by Gas Chromatography / Mass Spectrometry (GC/MS) analysis. Among the 13 PAHs, 12 of them, not including Benzo(e)pyrene (BeP), have been included in the priority pollutant list of the Clean Water Act of the United States Environmental Protection Agency (US EPA) since the 1970s.

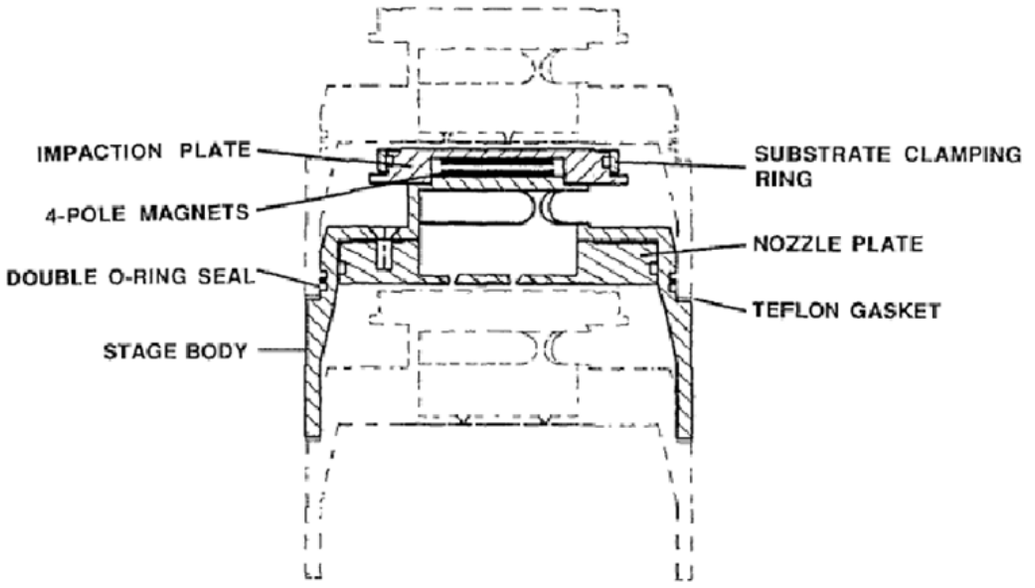



**Figure 4.** Schematic diagram of a MOUDI stage showing its relation to the above and below stages [19]

| Compound | Abbr. | Molecular formula | Molecular weight | No. of aromatic rings | Vapor pressure (Pa at 25 ºC) | Solubility in water (μg/L at 25 ºC) |
|---|---|---|---|---|---|---|
| Phenanthrene | Phe | $C_{14}H_{10}$ | 178 | 3 | $1.6\times10^{-2}$ | $1.3\times10^{3}$ |
| Anthracene | Ant | $C_{14}H_{10}$ | 178 | 3 | $8.0\times10^{-4}$ | 73 |
| Fluoranthene | Fluo | $C_{16}H_{10}$ | 202 | 4 | $1.2\times10^{-3}$ | 260 |
| Pyrene | Pyr | $C_{16}H_{10}$ | 202 | 4 | $6.0\times10^{-4}$ | 135 |
| Benzo(a)anthracene | BaA | $C_{18}H_{12}$ | 228 | 4 | $2.8\times10^{-5}$ | 5.6 |
| Chrysene | Chr | $C_{18}H_{12}$ | 228 | 4 | $8.4\times10^{-5}$ * | 2.0 |
| Benzo(b)fluoranthene | BbF | $C_{20}H_{12}$ | 252 | 5 | $6.7\times10^{-5}$ * | 0.80 |
| Benzo(k)fluoranthene | BkF | $C_{20}H_{12}$ | 252 | 5 | $1.3\times10^{-8}$ * | 0.76 |
| Benzo(e)pyrene | BeP | $C_{20}H_{12}$ | 252 | 5 | $7.6\times10^{-7}$ | 6.3 |
| Benzo(a)pyrene | BaP | $C_{20}H_{12}$ | 252 | 5 | $7.4\times10^{-7}$ | 3.8 |
| Indeno(1,2,3-cd)pyrene | IP | $C_{22}H_{12}$ | 276 | 6 | $1.3\times10^{-8}$ * | 62 |
| Dibenz(a,h)anthracene | DahA | $C_{22}H_{14}$ | 278 | 5 | $1.3\times10^{-8}$ * | 1.0 |
| Benzo(g,h,i)perylene | BghiP | $C_{20}H_{12}$ | 276 | 6 | $1.4\times10^{-8}$ | 0.26 |

*Pa at 20 ºC

**Table 1.** Physico-chemical properties of 13 PAHs measured in this study [2]

To monitor the temporal variations of total concentrations of particulate PAHs, photoelectric aerosol sensors (model PAS2000CE, EcoChem Analytics, Germany) [20] were used for real-time monitoring (Figure 5). Photoelectric aerosol sensors (PAS) work on the basis of photoelectric ionization of PAHs adsorbed onto particles [21]. The measurement techniques of this instrument have been described in detail elsewhere [22]. Briefly, a vacuum pump is used to draw ambient air through a quartz tube around which a UV lamp is mounted. Irradiation with UV light causes particles to emit electrons, which are then captured by surrounding gas molecules. Negatively charged particles are removed from the air stream,

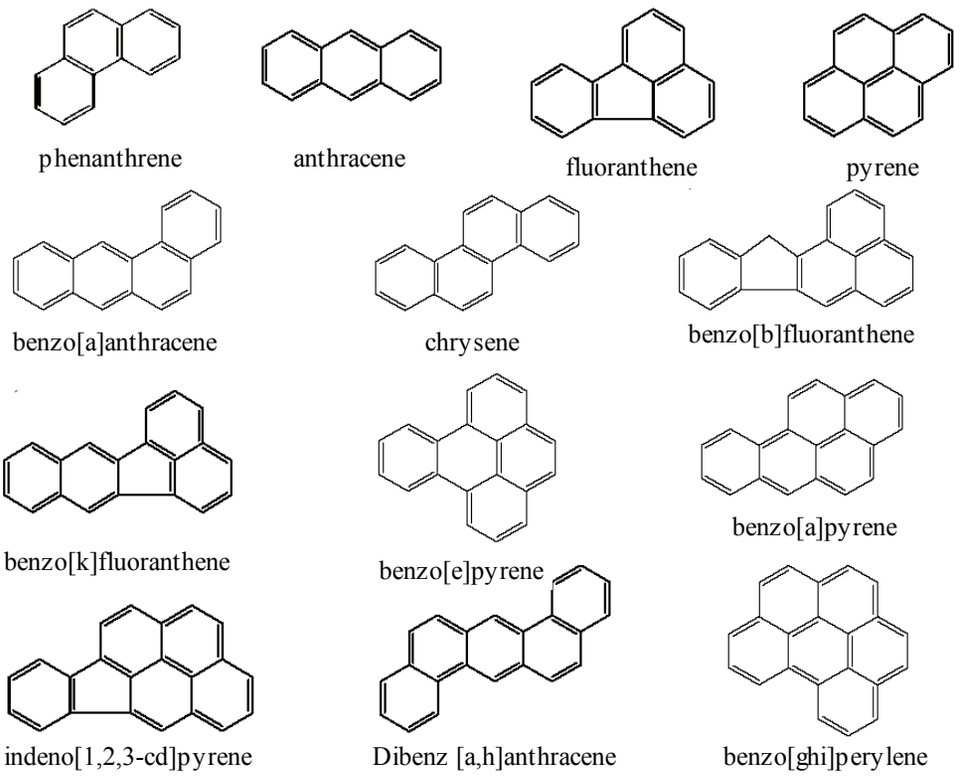



**Figure 5.** Structural formulas of the 13 PAHs

and the remaining positively charged particles are collected on a particle filter mounted in a Faraday cage. The particle filter converts the ion current to an electrical current, which is then amplified and measured with an electrometer (Figure 6). The electric current establishes signals that are proportional to the concentrations of total PAHs [20]. The target particle size is below 1 μm and the signals are recorded every 2 minutes. In the results of this study, PAS monitoring data are indicated as PAS signals without particular units, because the purpose of use of PAS is to know relative levels of temporal variations of total PAH concentrations, not to know absolute values of the total PAH concentrations, for which actual kinds of PAHs which compose the total concentrations cannot be identified by the PAS.

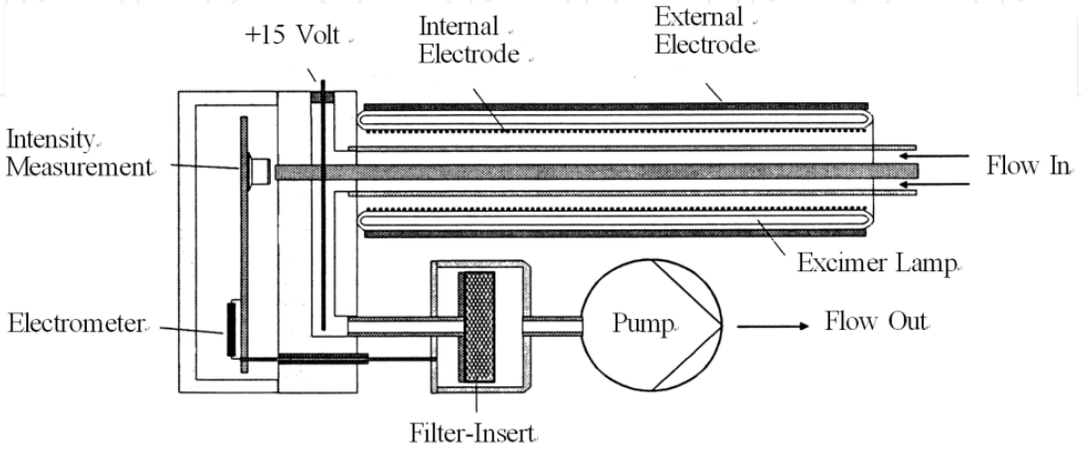



**Figure 6.** PAS2000CE




**Figure 7.** Scheme of PAS2000CE [49]

## 2.3. Particle size distribution

Particle sizes in the atmosphere are known to distribute with certain frequency modes, namely, nuclei mode, accumulation mode and coarse mode [23]. The nuclei mode, or ultrafine mode is mainly primary emission of vehicle exhaust and is carbonaceous particulate matter. The accumulation mode is responsible for formation of secondary organic aerosols especially through photochemical reactions with VOCs including gas phase PAHs and also for coagulation of particles. The coarse mode (>1.8 um) particles are mostly grown particles in the atmosphere and/or re-suspended road dust, which are reported to be subject to condensation of volatile materials including lighter PAHs. From previous studies, concentrations of PAHs are found to be highly dependent upon the size of particles. In view of association mechanisms and atmospheric processes of PAHs to urban aerosols, those particle size modes are applied to this study [7]. Based on previous studies on PAHs measurement using cascade air samplers (e.g., [24-25]) three particle size modes are defined for this study: ultrafine mode (< 0.18 μm), accumulation mode (0.18-1.8 μm) and coarse mode (1.8μm <) according to the particle cut sizes of the MOUDI.

## 2.4. Traffic and meteorological data

Road traffic was recorded using a video camera for 24 hours or shorter during the air sampling. The traffic volume was counted manually for 10 minutes in every hour, then multiplied by six to estimate hourly average volumes. At the CC site, hourly meteorological data monitored by the PCD were obtained. The meteorological data included temperature, solar radiation, relative humidity, rain, wind speed and wind direction. At the R6 site, wind speed and wind directions were monitored at 10-minute intervals using KADEC wind monitors (Kona Systems, Japan), and temperature, solar radiation, relative humidity and rainfall were monitored at 5-minute intervals using an AutoMet meteorology monitor (MET ONE Instruments, USA).

# 3. Diurnal variation of particle size distribution of PAHs

## 3.1. Preliminary measurement

One of the most influential and distinctive factors for diurnal PAH concentration variations was expected to be diurnal variations of vehicle emissions. Thus, it was considered most appropriate to investigate diurnal variations of particle size distributions of PAHs in accordance with morning and evening traffic peak hours and two off-peak hours in between, namely daytime and night time, in total four different time periods of the day for separate measurements. Preliminary PAS real-time monitoring was conducted to see if the PAS signals show morning and evening peaks corresponding to the traffic. The measurements were conducted from March 27th to April 2nd, 2006, at R6 and from April 21st to 23rd, 2006 at CC, right before the MOUDI air sampling, respectively. Figure 7 presents the results from the PAS signals. Although the timing of the PAS signal peaks were somewhat varied on different days, the morning and evening peak hours and the daytime and overnight off-peak hours were confirmed. Based on these observations, the following four time periods were decided for the MOUDI air sampling durations at each site to investigate diurnal variations of particle size distributions of PAHs: 6:00-10:00 (morning (m)), 12:00-16:00 (daytime (d)), 18:00-21:00 (evening (e)) and 22:00-5:00 (overnight (o)) at R6; and 6:00-9:30 (m), 13:00-17:00 (d), 18:30-21:30 (e) and 22:00-5:00 (o) at CC.

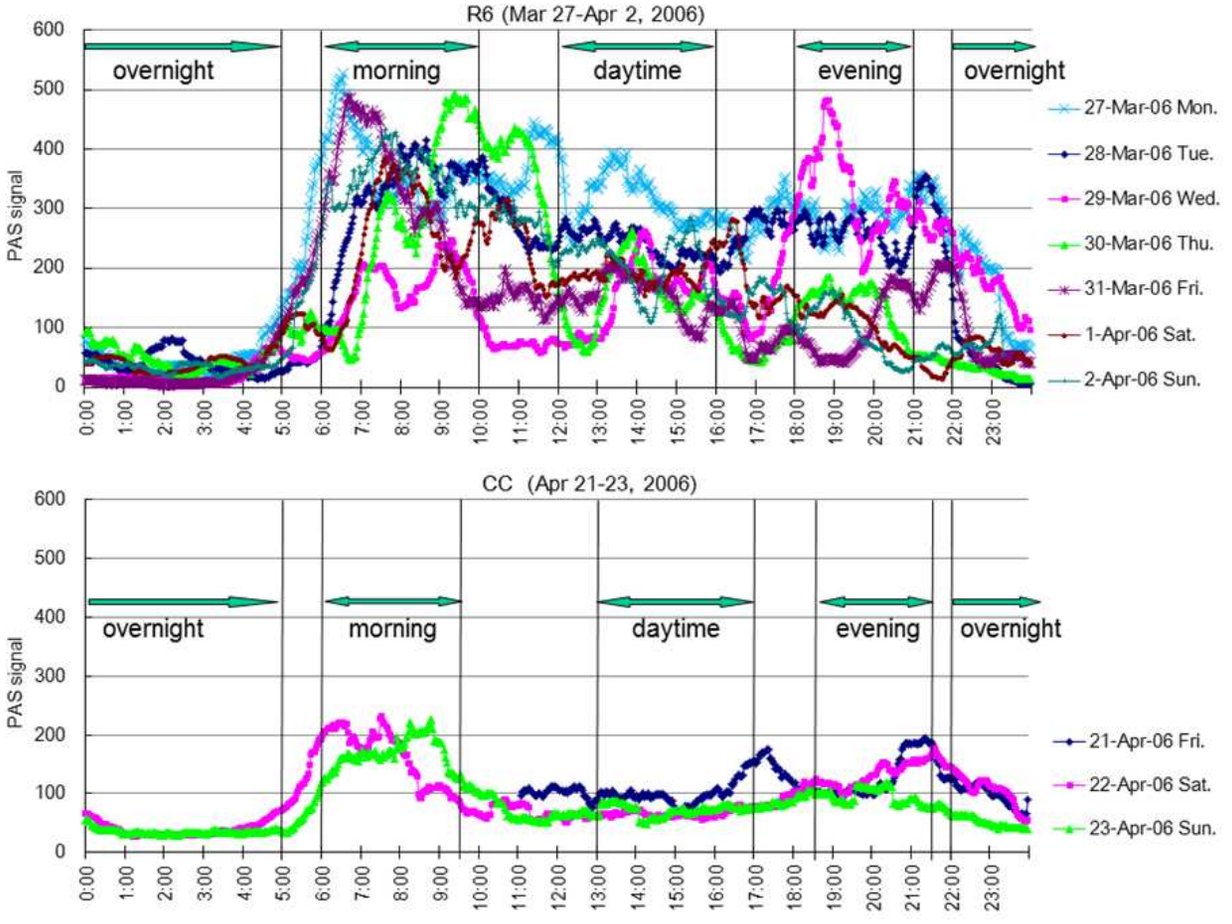



**Figure 8.** Preliminary real-time monitoring for the selection of four time periods corresponding to peak and off-peak hours of PAS signals for MOUDI air sampling [35]

## 3.2. Results and discussion

Air sampling was conducted using the MOUDI during the four selected time periods for three consecutive days. The sampling periods were April 3rd (Mon.)-6th (Thu.), 2006, at R6 and April 24th (Mon.)-27th (Thu.), 2006, at CC. Table 2 shows the 13 particle size-fractioned PAH concentrations (ng/m$^3$) during the four time periods of the day. Particulate matter was collected cumulatively on the same filters in each time period, while the air sampling using

| Time period | PAH | Particle size fraction ($\mu$m) | | | | | | | | | | Total | Detection limit |
|---|---|---|---|---|---|---|---|---|---|---|---|---|---|
| of day | | < 0.18 | 0.18～0.31 | 0.31～0.56 | 0.56～1.0 | 1.0～1.8 | 1.8～3.2 | 3.2～5.6 | 5.6～10 | 10～18 | 18 < | (ng/m$^3$) | (ng/m$^3$) |
| Morning | Phe | 0.064 | 0.072 | 0.061 | 0.026 | 0.020 | 0.017 | 0.0091 | 0.017 | 0.012 | 0.010 | 0.308 | 0.0015 |
| | Ant | 0.021 | 0.024 | 0.018 | 0.013 | 0.015 | 0.013 | 0.0060 | 0.012 | 0.0092 | 0.018 | 0.151 | 0.0015 |
| | Fluo | 0.065 | 0.074 | 0.054 | 0.024 | 0.017 | 0.014 | 0.0075 | 0.014 | 0.0090 | 0.0090 | 0.288 | 0.0015 |
| | Pyr | 0.12 | 0.13 | 0.097 | 0.042 | 0.030 | 0.022 | 0.010 | 0.020 | 0.013 | 0.014 | 0.497 | 0.0015 |
| | BaA | 0.074 | 0.094 | 0.065 | 0.023 | 0.014 | 0.012 | 0.007 | 0.014 | 0.013 | 0.012 | 0.329 | 0.0029 |
| | Chr | 0.079 | 0.11 | 0.086 | 0.033 | 0.021 | 0.014 | 0.009 | 0.019 | 0.015 | 0.016 | 0.400 | 0.0029 |
| | BbF | 0.19 | 0.17 | 0.15 | 0.046 | 0.017 | 0.014 | 0.010 | 0.017 | 0.013 | 0.015 | 0.642 | 0.0037 |
| | BkF | 0.10 | 0.11 | 0.078 | 0.039 | 0.018 | 0.0090 | 0.0089 | 0.012 | 0.0092 | 0.015 | 0.398 | 0.0037 |
| | BeP | 0.20 | 0.19 | 0.16 | 0.045 | 0.017 | 0.011 | 0.011 | 0.012 | N.D. | N.D. | 0.65 | 0.0018 |
| | BaP | 0.22 | 0.21 | 0.18 | 0.052 | 0.029 | 0.017 | 0.015 | 0.022 | N.D. | N.D. | 0.74 | 0.0037 |
| | IP | 0.14 | 0.11 | 0.086 | 0.034 | N.D. | N.D. | N.D. | N.D. | N.D. | N.D. | 0.37 | 0.0037 |
| | DahA | 0.023 | 0.010 | N.D. | N.D. | N.D. | N.D. | N.D. | N.D. | N.D. | N.D. | 0.033 | 0.015 |
| | BghiP | 0.27 | 0.19 | 0.18 | 0.059 | N.D. | N.D. | N.D. | N.D. | N.D. | N.D. | 0.69 | 0.0037 |
| | Σ13 PAHs | 1.6 | 1.5 | 1.2 | 0.44 | 0.20 | 0.14 | 0.094 | 0.16 | 0.094 | 0.109 | 5.5 | |
| | Ratio(%) | 28.4 | 26.9 | 22.1 | 7.9 | 3.6 | 2.6 | 1.7 | 2.9 | 1.7 | 2.0 | 100.0 | |
| Daytime | Phe | 0.042 | 0.097 | 0.11 | 0.049 | 0.045 | 0.039 | 0.032 | 0.033 | 0.039 | 0.034 | 0.51 | 0.0034 |
| | Ant | 0.023 | 0.045 | 0.053 | 0.030 | 0.057 | 0.037 | 0.028 | 0.027 | 0.035 | 0.033 | 0.37 | 0.0034 |
| | Fluo | 0.045 | 0.081 | 0.095 | 0.055 | 0.048 | 0.022 | 0.026 | 0.023 | 0.022 | 0.021 | 0.44 | 0.0034 |
| | Pyr | 0.075 | 0.16 | 0.18 | 0.091 | 0.067 | 0.032 | 0.034 | 0.032 | 0.028 | 0.027 | 0.73 | 0.0034 |
| | BaA | 0.048 | 0.086 | 0.095 | 0.059 | 0.055 | 0.027 | 0.047 | 0.024 | 0.038 | 0.032 | 0.51 | 0.0067 |
| | Chr | 0.073 | 0.10 | 0.12 | 0.058 | 0.061 | 0.039 | 0.059 | 0.038 | 0.048 | 0.038 | 0.64 | 0.0067 |
| | BbF | 0.11 | 0.21 | 0.22 | 0.079 | 0.048 | 0.040 | 0.045 | 0.033 | 0.039 | N.D. | 0.83 | 0.0084 |
| | BkF | 0.064 | 0.12 | 0.14 | 0.067 | 0.043 | 0.047 | 0.035 | 0.028 | 0.036 | N.D. | 0.58 | 0.0084 |
| | BeP | 0.077 | 0.19 | 0.21 | 0.053 | 0.023 | N.D. | 0.027 | N.D. | N.D. | N.D. | 0.58 | 0.0042 |
| | BaP | 0.099 | 0.18 | 0.17 | 0.049 | 0.064 | N.D. | 0.085 | N.D. | N.D. | N.D. | 0.65 | 0.0084 |
| | IP | 0.19 | 0.21 | 0.24 | N.D. | N.D. | N.D. | N.D. | N.D. | N.D. | N.D. | 0.64 | 0.0084 |
| | DahA | N.D. | N.D. | N.D. | N.D. | N.D. | N.D. | N.D. | N.D. | N.D. | N.D. | N.D. | 0.034 |
| | BghiP | 0.23 | 0.26 | 0.27 | 0.035 | N.D. | N.D. | N.D. | N.D. | N.D. | N.D. | 0.80 | 0.0084 |
| | Σ13 PAHs | 1.1 | 1.7 | 1.9 | 0.63 | 0.51 | 0.28 | 0.42 | 0.24 | 0.29 | 0.19 | 7.3 | |
| | Ratio(%) | 14.8 | 23.9 | 26.2 | 8.6 | 7.0 | 3.9 | 5.8 | 3.3 | 3.9 | 2.6 | 100.0 | |
| Evening | Phe | 0.050 | 0.096 | 0.096 | 0.049 | 0.036 | 0.036 | 0.037 | 0.038 | 0.035 | 0.032 | 0.50 | 0.0028 |
| | Ant | 0.029 | 0.053 | 0.046 | 0.031 | 0.028 | 0.037 | 0.030 | 0.031 | 0.035 | 0.025 | 0.35 | 0.0028 |
| | Fluo | 0.058 | 0.10 | 0.084 | 0.054 | 0.034 | 0.039 | 0.035 | 0.030 | 0.033 | 0.027 | 0.49 | 0.0028 |
| | Pyr | 0.075 | 0.18 | 0.15 | 0.075 | 0.042 | 0.059 | 0.052 | 0.040 | 0.034 | 0.030 | 0.73 | 0.0028 |
| | BaA | 0.073 | 0.11 | 0.12 | 0.035 | 0.039 | 0.032 | 0.037 | 0.033 | 0.036 | 0.039 | 0.55 | 0.0056 |
| | Chr | 0.076 | 0.15 | 0.11 | 0.048 | 0.037 | 0.034 | 0.033 | 0.038 | 0.033 | 0.036 | 0.60 | 0.0056 |
| | BbF | 0.12 | 0.25 | 0.23 | 0.051 | 0.053 | 0.029 | 0.033 | 0.037 | 0.041 | 0.033 | 0.89 | 0.0070 |
| | BkF | 0.13 | 0.17 | 0.13 | 0.047 | 0.063 | 0.033 | 0.035 | 0.027 | 0.027 | 0.030 | 0.69 | 0.0070 |
| | BeP | 0.10 | 0.17 | 0.22 | 0.051 | N.D. | 0.022 | 0.021 | N.D. | N.D. | N.D. | 0.58 | 0.0035 |
| | BaP | 0.10 | 0.25 | 0.30 | 0.12 | N.D. | 0.062 | 0.050 | N.D. | N.D. | N.D. | 0.89 | 0.0070 |
| | IP | 0.19 | 0.20 | 0.15 | 0.033 | N.D. | N.D. | N.D. | N.D. | N.D. | N.D. | 0.57 | 0.0070 |
| | DahA | 0.049 | 0.080 | N.D. | N.D. | N.D. | N.D. | N.D. | N.D. | N.D. | N.D. | 0.13 | 0.028 |
| | BghiP | 0.29 | 0.30 | 0.26 | 0.055 | N.D. | N.D. | N.D. | N.D. | N.D. | N.D. | 0.90 | 0.0070 |
| | Σ13 PAHs | 1.3 | 2.1 | 1.9 | 0.65 | 0.33 | 0.38 | 0.36 | 0.27 | 0.27 | 0.25 | 7.9 | |
| | Ratio(%) | 17.1 | 26.9 | 23.9 | 8.2 | 4.2 | 4.9 | 4.6 | 3.5 | 3.5 | 3.2 | 100.0 | |
| Overnight | Phe | 0.017 | 0.036 | 0.031 | 0.020 | 0.021 | 0.014 | 0.013 | 0.019 | 0.011 | 0.013 | 0.20 | 0.0010 |
| | Ant | 0.0088 | 0.017 | 0.013 | 0.011 | 0.011 | 0.012 | 0.010 | 0.022 | 0.0071 | 0.010 | 0.122 | 0.0010 |
| | Fluo | 0.014 | 0.027 | 0.026 | 0.016 | 0.020 | 0.012 | 0.014 | 0.032 | 0.0074 | 0.010 | 0.177 | 0.0010 |
| | Pyr | 0.028 | 0.052 | 0.049 | 0.031 | 0.038 | 0.023 | 0.018 | 0.037 | 0.011 | 0.013 | 0.30 | 0.0010 |
| | BaA | 0.024 | 0.034 | 0.031 | 0.014 | 0.015 | 0.0083 | 0.016 | 0.031 | 0.0077 | 0.011 | 0.190 | 0.0021 |
| | Chr | 0.023 | 0.043 | 0.039 | 0.026 | 0.024 | 0.014 | 0.014 | 0.031 | 0.0070 | 0.010 | 0.231 | 0.0021 |
| | BbF | 0.022 | 0.055 | 0.053 | 0.012 | 0.027 | 0.013 | 0.018 | 0.028 | 0.011 | 0.012 | 0.25 | 0.0026 |
| | BkF | 0.032 | 0.058 | 0.070 | 0.031 | 0.033 | 0.0094 | 0.020 | 0.030 | 0.011 | 0.013 | 0.307 | 0.0026 |
| | BeP | 0.035 | 0.086 | 0.082 | 0.035 | 0.033 | 0.012 | 0.016 | 0.012 | 0.0086 | 0.011 | 0.329 | 0.0013 |
| | BaP | 0.041 | 0.112 | 0.099 | 0.049 | 0.027 | 0.019 | 0.029 | 0.023 | 0.011 | 0.013 | 0.42 | 0.0026 |
| | IP | 0.065 | 0.067 | 0.083 | 0.032 | 0.019 | N.D. | N.D. | 0.017 | N.D. | N.D. | 0.28 | 0.0026 |
| | DahA | 0.017 | N.D. | N.D. | N.D. | N.D. | N.D. | N.D. | N.D. | N.D. | N.D. | 0.017 | 0.010 |
| | BghiP | 0.11 | 0.11 | 0.11 | 0.044 | 0.030 | 0.009 | 0.012 | 0.027 | 0.010 | 0.021 | 0.48 | 0.0026 |
| | Σ13 PAHs | 0.436 | 0.69 | 0.68 | 0.32 | 0.30 | 0.145 | 0.18 | 0.31 | 0.102 | 0.14 | 3.3 | |
| | Ratio(%) | 13.2 | 21.0 | 20.7 | 9.8 | 9.0 | 4.4 | 5.4 | 9.3 | 3.1 | 4.1 | 100.0 | |

(a)

| Time period of day | PAH | Particle size fraction ($\mu$m) < 0.18 | 0.18～0.31 | 0.31～0.56 | 0.56～1.0 | 1.0～1.8 | 1.8～3.2 | 3.2～5.6 | 5.6～10 | 10～18 | 18 < | Total (ng/m$^3$) | Detection limit (ng/m$^3$) |
|---|---|---|---|---|---|---|---|---|---|---|---|---|---|
| Morning | Phe | 0.051 | 0.077 | 0.070 | 0.044 | 0.039 | 0.037 | 0.039 | 0.034 | 0.036 | 0.035 | 0.46 | 0.0035 |
| | Ant | 0.020 | 0.021 | 0.019 | 0.018 | 0.017 | 0.016 | 0.021 | 0.016 | 0.019 | 0.020 | 0.19 | 0.0035 |
| | Fluo | 0.031 | 0.040 | 0.046 | 0.026 | 0.023 | 0.020 | 0.022 | 0.016 | 0.022 | 0.019 | 0.27 | 0.0035 |
| | Pyr | 0.058 | 0.069 | 0.068 | 0.040 | 0.029 | 0.027 | 0.025 | 0.022 | 0.022 | 0.023 | 0.38 | 0.0035 |
| | BaA | 0.031 | 0.030 | 0.023 | 0.019 | 0.018 | 0.016 | 0.024 | 0.010 | 0.014 | 0.025 | 0.21 | 0.0070 |
| | Chr | 0.057 | 0.061 | 0.048 | 0.025 | 0.021 | 0.020 | 0.023 | 0.022 | 0.032 | 0.034 | 0.34 | 0.0070 |
| | BbF | 0.094 | 0.13 | 0.12 | 0.11 | N.D. | N.D. | N.D. | N.D. | N.D. | N.D. | 0.46 | 0.0087 |
| | BkF | 0.093 | 0.079 | 0.069 | 0.038 | N.D. | N.D. | N.D. | N.D. | N.D. | N.D. | 0.28 | 0.0087 |
| | BeP | 0.10 | 0.17 | 0.13 | 0.039 | N.D. | N.D. | N.D. | N.D. | N.D. | N.D. | 0.45 | 0.0044 |
| | BaP | 0.10 | 0.14 | 0.10 | 0.036 | N.D. | N.D. | N.D. | N.D. | N.D. | N.D. | 0.38 | 0.0087 |
| | IP | 0.059 | 0.11 | 0.058 | N.D. | N.D. | N.D. | N.D. | N.D. | N.D. | N.D. | 0.23 | 0.0087 |
| | DahA | N.D. | N.D. | N.D. | N.D. | N.D. | N.D. | N.D. | N.D. | N.D. | N.D. | N.D. | 0.035 |
| | BghiP | 0.13 | 0.20 | 0.15 | N.D. | N.D. | N.D. | N.D. | N.D. | N.D. | N.D. | 0.48 | 0.0087 |
| | Σ13 PAHs | 0.84 | 1.1 | 0.91 | 0.39 | 0.15 | 0.14 | 0.15 | 0.12 | 0.14 | 0.16 | 4.1 | |
| | Ratio(%) | 20.2 | 27.5 | 22.0 | 9.5 | 3.6 | 3.3 | 3.7 | 2.9 | 3.5 | 3.8 | 100.0 | |
| Daytime | Phe | 0.050 | 0.072 | 0.082 | 0.042 | 0.039 | 0.039 | 0.038 | 0.033 | 0.047 | 0.044 | 0.48 | 0.0032 |
| | Ant | 0.024 | 0.026 | 0.034 | 0.024 | 0.018 | 0.022 | 0.022 | 0.014 | 0.024 | 0.022 | 0.23 | 0.0032 |
| | Fluo | 0.037 | 0.050 | 0.051 | 0.033 | 0.023 | 0.024 | 0.019 | 0.014 | 0.026 | 0.030 | 0.31 | 0.0032 |
| | Pyr | 0.050 | 0.081 | 0.073 | 0.049 | 0.032 | 0.035 | 0.029 | 0.016 | 0.028 | 0.021 | 0.42 | 0.0032 |
| | BaA | 0.042 | 0.045 | 0.044 | 0.026 | 0.020 | 0.028 | 0.030 | 0.015 | 0.027 | 0.028 | 0.31 | 0.0064 |
| | Chr | 0.059 | 0.054 | 0.044 | 0.025 | 0.014 | 0.023 | 0.018 | 0.014 | 0.025 | 0.020 | 0.30 | 0.0064 |
| | BbF | 0.11 | 0.12 | 0.086 | 0.055 | 0.041 | 0.028 | N.D. | 0.032 | 0.040 | 0.046 | 0.56 | 0.0081 |
| | BkF | 0.057 | 0.045 | 0.059 | 0.028 | 0.018 | 0.017 | N.D. | 0.021 | 0.023 | 0.018 | 0.29 | 0.0081 |
| | BeP | 0.11 | 0.10 | 0.097 | 0.032 | N.D. | N.D. | N.D. | N.D. | 0.024 | 0.025 | 0.40 | 0.0040 |
| | BaP | 0.056 | 0.055 | 0.061 | 0.012 | N.D. | N.D. | N.D. | N.D. | 0.030 | N.D. | 0.21 | 0.0081 |
| | IP | 0.052 | 0.128 | 0.099 | N.D. | N.D. | N.D. | N.D. | N.D. | N.D. | N.D. | 0.28 | 0.0081 |
| | DahA | N.D. | N.D. | N.D. | N.D. | N.D. | N.D. | N.D. | N.D. | N.D. | N.D. | N.D. | 0.032 |
| | BghiP | 0.070 | 0.14 | 0.11 | 0.030 | N.D. | N.D. | N.D. | N.D. | N.D. | N.D. | 0.35 | 0.0081 |
| | Σ13 PAHs | 0.72 | 0.92 | 0.84 | 0.36 | 0.21 | 0.22 | 0.16 | 0.16 | 0.29 | 0.25 | 4.1 | |
| | Ratio(%) | 17.6 | 22.2 | 20.5 | 8.6 | 5.0 | 5.3 | 3.8 | 3.8 | 7.1 | 6.2 | 100.0 | |
| Evening | Phe | 0.048 | 0.070 | 0.086 | 0.064 | 0.053 | 0.042 | 0.042 | 0.033 | 0.035 | 0.033 | 0.51 | 0.0038 |
| | Ant | 0.018 | 0.025 | 0.034 | 0.031 | 0.022 | 0.026 | 0.021 | 0.022 | 0.023 | 0.020 | 0.24 | 0.0038 |
| | Fluo | 0.030 | 0.048 | 0.059 | 0.040 | 0.028 | 0.027 | 0.024 | 0.023 | 0.020 | 0.018 | 0.32 | 0.0038 |
| | Pyr | 0.050 | 0.082 | 0.080 | 0.051 | 0.044 | 0.041 | 0.032 | 0.026 | 0.030 | 0.021 | 0.46 | 0.0038 |
| | BaA | 0.006 | 0.036 | 0.033 | 0.030 | 0.029 | 0.020 | 0.031 | 0.020 | 0.023 | 0.033 | 0.26 | 0.0076 |
| | Chr | 0.008 | 0.049 | 0.048 | 0.029 | 0.027 | 0.020 | 0.024 | 0.025 | 0.020 | 0.019 | 0.27 | 0.0076 |
| | BbF | 0.10 | 0.12 | 0.11 | 0.051 | 0.039 | 0.031 | N.D. | N.D. | N.D. | N.D. | 0.45 | 0.0094 |
| | BkF | 0.038 | 0.050 | 0.060 | 0.035 | 0.023 | 0.015 | N.D. | N.D. | N.D. | N.D. | 0.22 | 0.0094 |
| | BeP | 0.096 | 0.12 | 0.12 | 0.044 | 0.041 | N.D. | N.D. | N.D. | N.D. | N.D. | 0.41 | 0.0047 |
| | BaP | 0.077 | 0.075 | 0.087 | 0.054 | 0.057 | N.D. | N.D. | N.D. | N.D. | N.D. | 0.35 | 0.0094 |
| | IP | 0.044 | 0.082 | 0.10 | N.D. | N.D. | N.D. | N.D. | N.D. | N.D. | N.D. | 0.23 | 0.0094 |
| | DahA | N.D. | N.D. | N.D. | N.D. | N.D. | N.D. | N.D. | N.D. | N.D. | N.D. | N.D. | 0.038 |
| | BghiP | 0.065 | 0.11 | 0.14 | N.D. | N.D. | N.D. | N.D. | N.D. | N.D. | N.D. | 0.32 | 0.0094 |
| | Σ13 PAHs | 0.58 | 0.87 | 0.95 | 0.43 | 0.36 | 0.22 | 0.17 | 0.15 | 0.15 | 0.14 | 4.0 | |
| | Ratio(%) | 14.4 | 21.5 | 23.6 | 10.6 | 9.0 | 5.5 | 4.3 | 3.7 | 3.7 | 3.6 | 100.0 | |
| Overnight | Phe | | | | | | | | | | | 0.45 | 0.0026 |
| | Ant | | | | | | | | | | | 0.28 | 0.0026 |
| | Fluo | | | | | | | | | | | 0.33 | 0.0026 |
| | Pyr | | | | | | | | | | | 0.41 | 0.0026 |
| | BaA | | | | | | | | | | | 0.24 | 0.0051 |
| | Chr | | | | | *data not available* | | | | | | 0.35 | 0.0051 |
| | BbF | | | | | | | | | | | 0.42 | 0.0064 |
| | BkF | | | | | | | | | | | 0.25 | 0.0064 |
| | BeP | | | | | | | | | | | 0.25 | 0.0032 |
| | BaP | | | | | | | | | | | 0.24 | 0.0064 |
| | IP | | | | | | | | | | | 0.07 | 0.0064 |
| | DahA | | | | | | | | | | | N.D. | 0.026 |
| | BghiP | | | | | | | | | | | 0.22 | 0.0064 |
| | Σ13 PAHs | | | | | | | | | | | 3.5 | |
| | Ratio(%) | | | | | | | | | | | | |

(b)

**Table 2.** Particle size-fractioned 13 PAHs concentrations (ng/m$^3$) in the four time periods of the day a) Rama6; b) Chockchai4

the MOUDI was repeated for three consecutive days. After the sampling on the first and second days, the filters were kept in plastic cases and carried until the sampling on the second and third days. (N.B. Unfortunately, filter samples of CC overnight were mishandled and size-segregated PAH concentration data and particle weight data are not available. However, total atmospheric PAH concentrations are available using the amount of air pumped in by the MOUDI equipment as shown in Table 2.)

Concurrent with the three-day air sampling using the MOUDI, PAS real-time monitoring was also conducted using the PASs, which showed similar trends of diurnal variations to those observed in the preliminary measurements. At R6, the PAH signal values sharply increased from approximately 5 am and reached morning peaks between 9 and 10 am during the three days. Daytime concentrations were lower than in the morning. In the daytime and evening, several small peaks appeared. From around midnight to 5 am, concentrations were remarkably low. At CC, sharp morning peaks were observed at approximately 7 am on April 24th and around 8 am on April 27th. In the evening, broader peaks appeared between 4 and 9 pm, and then the concentration decreased. The sharp increase in the morning was observed at both sites. This observation is consistent with that in previous reports [12,15-16]. The sharp morning peaks can be explained by both the strong atmospheric stability caused by the inversion layer and an increase in emissions from the morning traffic. Although the total traffic volume was smaller at R6 (74,000 vehicle/day on April 5th (Mon.)) than that at CC (92,000 vehicle/day on April 24th (Wed.)), higher concentrations were observed at R6 throughout the day, possibly due to the covered configuration that restricted the atmospheric dilution effect. According to the traffic monitoring, congestion occurred during the daytime at both sites, but daytime PAS signal levels at CC were constantly low compared with the large fluctuations of the daytime levels at R6.

Table 3 shows the average local meteorological data during the three-day monitoring periods. At both sites, the mean wind directions were almost stable at southwest, which situates the both sampling locations at downwind of the road emissions. At R6, the wind speed, which ranged from 0.2-0.6 m/s, was low compared with that at CC. The observation implies the limited dispersion and long residence time of airborne PAHs within the site. On the other hand, the wind speed at CC was much higher, ranging 1.3-2.8 m/s, implying faster dispersion. Solar radiation, which promotes photochemical decomposition of PAHs [26], was more than 40% lower at R6 throughout the day because of the elevated highway and the large buildings along the R6 road. This road configuration may also explain the higher daytime concentrations at R6.

| | Temperature (°C) | | | | Solar radiation (W/m²) | | | | Relative humidity (%) | | | |
|---|---|---|---|---|---|---|---|---|---|---|---|---|
| | m | d | e | o | m | d | e | o | m | d | e | o |
| R6 | 29.5 | 35.9 | 31.2 | 29.7 | 26.1 | 284.8 | 0.2 | 0 | 85.3 | 57.9 | 76.3 | 83.8 |
| CC | 27.9 | 29.1 | 29.6 | 28.0 | 129.3 | 762.5 | 12.7 | 0.4 | 69.5 | 61.9 | 55.9 | 68.2 |
| | Wind speed (m/s) | | | | Wind direction | | | | | | | |
| | m | d | e | o | m | d | e | o | | | | |
| R6 | 0.2 | 0.6 | 0.3 | 0.5 | SW | WSW | SW | W | | | | |
| CC | 1.9 | 1.3 | 1.8 | 2.8 | SSW | SSW | SSW | SW | | | | |

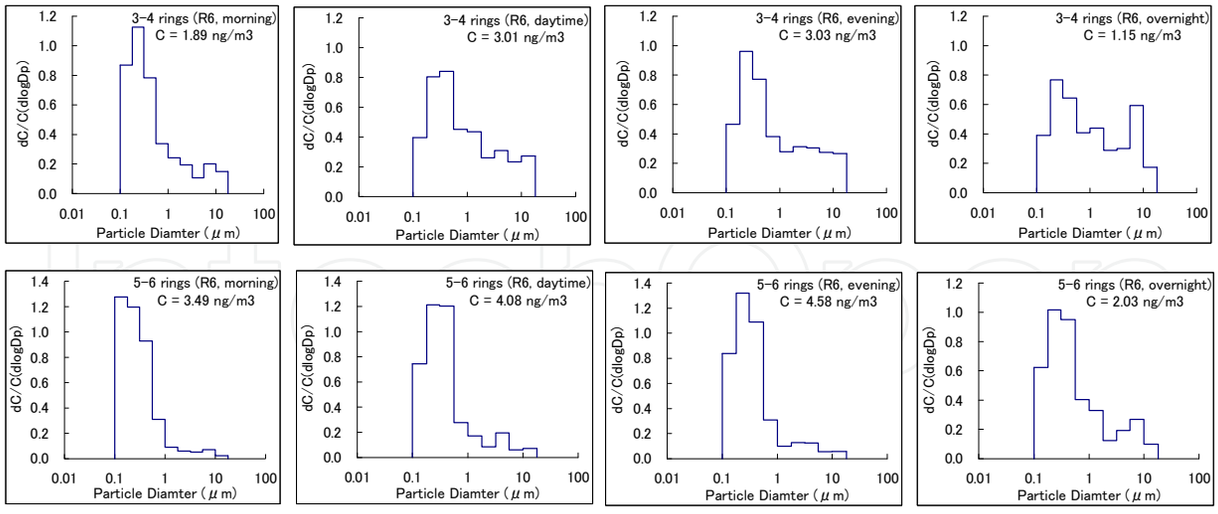
**Table 3.** Table 3. Local meteorological data; average during the four time periods of the day (April 3-6th, 2006 at R6 and April 24-27th, 2006 at CC).

Diurnal variations of particle size distribution of the 13 PAHs concentrations are shown in Figure 8 with classification of semi-volatile 3-4 ring PAHs and non-volatile 5-6 ring PAHs, respectively. Each graph of the size distribution is shown as Lungren type plots [27]. An overall trend of the size distribution was consistent with that in previous studies that concentrations of PAHs were found to be highly dependent upon the size of particulate matter, with the greatest concentrations being the submicron size range (e.g., [7, 28-30]). The higher concentrations at the submicron range can be explained by the condensation mechanism because larger specific surface areas are associated with such particles (e.g., [31]). On the other hand, there were clear differences of the size distribution between the groups of 3-4 ring and 5-6 ring PAHs. Contribution of coarser, or above 1μm range, was larger for 3-4 ring PAHs, while 5-6 ring PAHs were dominantly distributed in the finer size ranges at both of the sites, regardless of the time periods. The results regarding the relationship of PAH size distribution between ring number of PAHs and associated particle size were consistent with that in many other studies conducted previously, not only at Bangkok but also at various places (e.g., [7,13,32]). The Kelvin effect explains this trend. It determines the relationship between the particle diameter and vapor pressure, where more volatile species, namely lower weight PAHs, are associated with larger diameter particles.

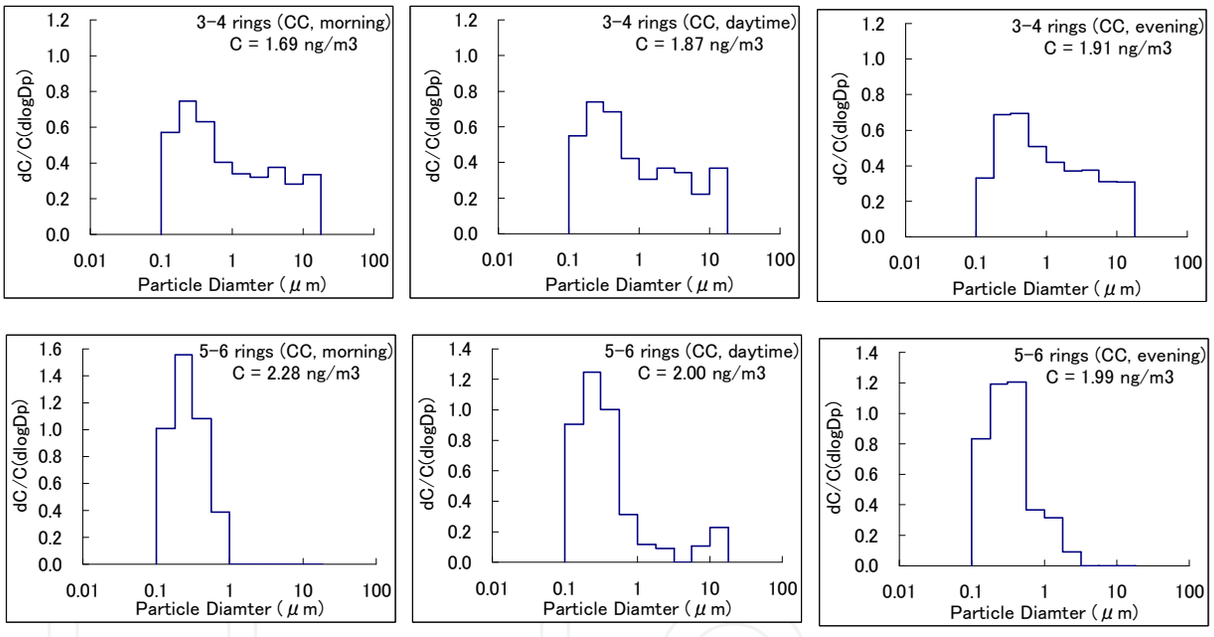
In terms of the temporal variations of PAH size distribution, at R6 in the morning, the distribution of 3-4 ring PAHs had a peak in the 0.18-0.31μm range, while the distribution of 5-6 ring PAHs had a peak in the finest range of below 0.18μm. The ratios of the ultrafine mode were clearly higher than those of other time periods, indicating an elevated burden of primary vehicle exhaust emission in the morning rush. From the morning to daytime, the distribution of both 3-4 ring and 5-6 ring PAHs slightly shifted to a coarser range. It implies atmospheric processes of particles, such as coagulation, condensation and photochemical reactions, which lead to growth of particles under stronger solar radiation and less vehicle emissions in the daytime. In the evening, the distribution peaks shifted back to finer ranges possibly due to traffic increase again in the evening rush. In the nighttime, distribution in coarser range increased apparently, possibly due to increased re-suspension of road dust caused by a faster driving speed of motor vehicles.

At CC, as a whole the coarser range contributed more than that at R6. This may be due to faster wind speed at CC enhancing re-suspension of coarse particles and/or faster dispersion of fine particles because of the open-space configuration of the road. Unlike at R6, any explicable trend of diurnal variations of the size distributions could not be identified at CC, rather some fluctuation of the size distribution was observed. This could be due to shorter residence time of particles in the site by the faster dispersion because of the open-structure configuration and faster wind, so atmospheric processes of particle growth might be limited compared to the R6's case.

To further support the discussion of diurnal variations of size distribution of PAHs, PAH contents in particulate matter (μg/g) were analyzed according to the three particle size modes in the four time periods of day (Figure 9). (N.B. Figure 8 showed PAH concentrations per unit air mass.) The PAH contents varied considerably according to the particle size modes and the different time periods. In general, smaller particle size modes had higher




(a)

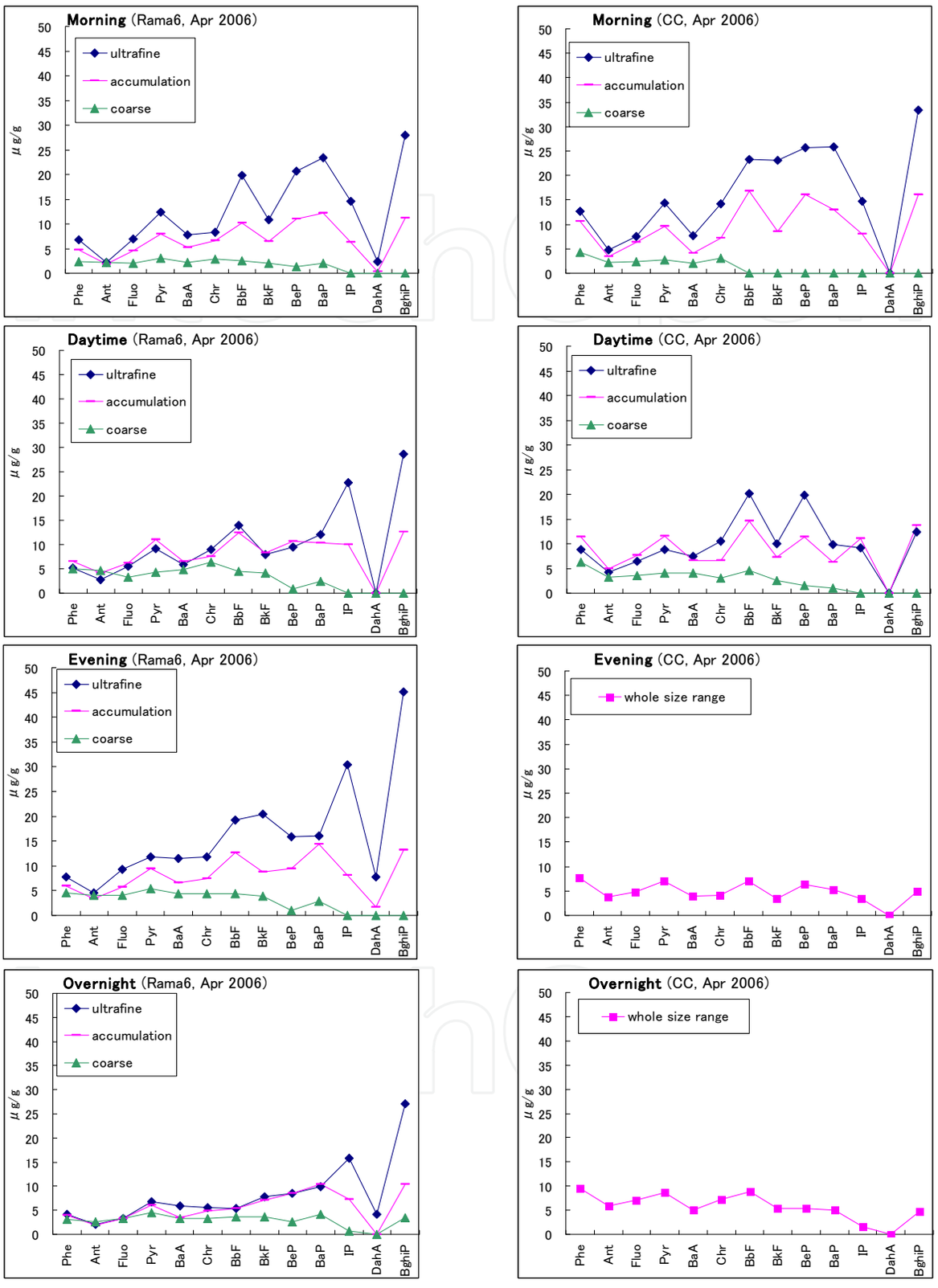



(b)

**Figure 9.** Size distributions of 3-4 ring and 5-6 ring PAH concentrations in the four time periods of day. a) Rama6; b) Chockchai4

PAH contents. An exceptional case was that low molecular PAHs up to Pyrene in the accumulation mode showed higher contents than those in the ultrafine mode in the daytime at both sites. It might again imply accelerated accumulation processes in the daytime. For example, accumulation mode particles went through photochemical reactions with VOCs accompanying condensation of low molecular weight gaseous phase PAHs in the daytime.

According to previous reports [33-34] Zielinska (2004), elevated concentrations of high molecular weight PAHs, especially BghiP, indicate significant contribution of gasoline exhaust. As shown in the figure, BghiP content in the ultrafine mode were remarkably high in all the four time periods at R6 and in the morning at CC, again implying significant




N.B.) The particulate weight data of the ultrafine mode for CC evening, and size distribution data of particle weight for CC overnight were not obtained, thus their mode distribution data are not available in the figure.

**Figure 10.** 13 PAH contents in the three particle modes in the four time periods of day (ultrafine: < 0.18μm, accumulation: 0.18-1.8μm, coarse: 1.8μm <)

contribution of gasoline vehicles to the roadside atmospheric PAHs. Especially the BghiP content in the ultrafine mode in the evening at R6 had the highest value. In fact at this time period, the ratio of the gasoline vehicles to the total traffic volume was the highest (63%) among the four time periods at the two sites.

## 4. Conclusion

This study clearly showed diurnal variations of particle size distribution of PAHs in four different time periods of day by field measurements on the two different types of roads in Bangkok, Thailand. The data indicated possible influences on the temporal variations of size distribution of PAHs by diurnal changes in traffic emissions, road configurations in relation to dispersion efficiency, meteorological conditions, atmospheric processes of particles such as coagulation, condensation and photochemical reactions under daytime sunlight, also atmospheric processes of PAHs in the accumulation particle mode. In view of people's exposure to vehicular emissions in an urban area with heavy road traffic, it is desired that urban air quality monitoring should be conducted in more comprehensive ways with higher resolutions of time and space, and actual behavior of pollutants be elucidated by various advanced approaches.

## Author details

Tomomi Hoshiko*
*Department of Urban Engineering, Graduate School of Engineering, The University of Tokyo, Tokyo, Japan*

Kazuo Yamamoto and Fumiyuki Nakajima
*Environmental Science Center, The University of Tokyo, Tokyo, Japan*

Tassanee Prueksasit
*Department of Environmental Science, Faculty of Science, Chulalongkorn University, Bangkok, Thailand*

## 5. References

[1] IARC (2011) IARC monographs on the evaluation of carcinogenic risks to humans. http://monographs.iarc.fr/ENG/Classification/index.php. Accessed 13 Apr 2012.
[2] IPCS (1998) Selected non-heterocyclic polycyclic aromatic hydrocarbons. Environmetal Health Criteria 202. WHO, Geneva.
[3] Beak SO, Field RA, Goldstone ME, Kirk PW, Lester JN, Perry R (1991) A review of atmospheric polycyclic aromatic hydrocarbons: Sources, fate and behavior. Water Air and Soil Pollution 60: 279-300.
[4] European Commission (2001) Ambient air pollution by Polycyclic Aromatic Hydrocarbons (PAH). Position Paper.

* Corresponding Author

[5] Nielsen T (1996) Traffic contribution of polycyclic aromatic hydrocarbons in the center of a large city. Atmospheric Environment 30: 3481-3490.
[6] Panther B, Hooper M, Limpaseni W, Hooper B (1996) Polycyclic aromatic hydrocarbon as environmental contaminants: Some results from Bangkok. The third international symposium of ETERNET-APR: Conservation of the hydrospheric environment. Bangkok. December 1996.
[7] Venkataraman C, Thomas S, Kulkarni P (1999) Size distributions of polycylic aromatic hydrocarbons – Gas/particle partitioning to urban aerosols. Journal of Aerosol Science 30: 759-770.
[8] Pollution Control Department, Ministry of Natural Resources and Environment, Thailand (2010) Thailand State of Pollution Report 2010.
[9] European Environment Agency (2004) Air pollution in Europe 1990-2000. Topic report.
[10] Panther B, Hooper MA, Tapper NJ (1999) A comparison of air particulate matter and associated polycyclic aromatic hydrocarbons in some tropical and temperate urban environments. Atmospheric Environment 33: 4087-4099.
[11] Garivait H, Polprasert C, Yoshizumi K, Reutergardh LB (2001) Airborne polycyclic aromatic hydrocarbons (PAH) in Bangkok urban air: Part II. Level and distribution. Polycyclic Aromatic Compounds 18: 325-350.
[12] Chetwittayachan T, Shimazaki D, Yamamoto K (2002) A comparison of temporal variation of particle-bound polycyclic aromatic hydrocarbons (pPAHs) concentration in different urban environments: Tokyo, Japan, and Bangkok, Thailand. Atmospheric Environment 36: 2027-2037.
[13] Boonyatumanond R, Murakami M, Wattayakorn G, Togo A, Takada H (2007) Sources of polycyclic aromatic hydrocarbons (PAHs) in street dust in a tropical Asian megacity, Bang-kok, Thailand. The Science of the Total Environment 384: 420-432.
[14] Nielsen T, Jorgensen HE, Larsen JC, Poulen M (1996) City air pollution of polycyclic aromatic hydrocarbons and other mutagens: occurrence, sources and health effects. The Science of the Total Environment 189/190: 41-49
[15] Chetwittayachan T (2002) Temporal variation of particle-bound polycyclic aromatic hydro-carbons (pPAHs) concentration and risk assessment of their possible human exposure in urban air environments. PhD thesis submitted to department of urban engineering, graduate school of engineering, The University of Tokyo
[16] Chetwittayachan T, Kido R, Shimazaki D, Yamamoto K (2002) Diurnal profiles of particle-bound polycyclic aromatic hydrocarbon (pPAH) concentration in urban environment in To-kyo metropolitan area. Water, Air, and Soil Pollution: Focus 2: 203-221
[17] Fine PM, Chakrabarti B, Krudysz M, Schauer JJ, Sioutas C (2004) Diurnal Variations of Individual Organic Compound Constituents of Ultrafine and Accumulation Mode Particulate Matter in the Los Angeles Basin. Environmental Science and Technology 38: 1296-1304.
[18] MSP Corporation (1998) Micro-Orifice Uniform Deposit Impactor Instruction Manual, Model 100/ Model 110

[19] Marple VA, Rubow KL, Behm, SM (1991) A microorifice uniform deposit impactor (MOUDI): Description, calibration and use. Aerosol Science and Technology 14: 434-446.
[20] EcoChem Analytics (1999) User's guide: Realtime PAH monitor PAS2000CE.
[21] Burtscher H, Schmidt-Ott A (1986) In situ measurement of adsorption and condensation of a polycyclic aromatic hydrocarbon on ultrafine c particles by means of photoemission. Journal of Aerosol Science 17: 699-703.
[22] Burtscher H (1992) Measurement and characteristics of combustion aerosols with special consideration of photoelectric charging and charging by flame ions. Journal of Aerosol Science 23: 549-595.
[23] Kittelson DB (1998) Engines and Nanoparticles: A Review, J. Aerosol. Sci. 29:575–588.
[24] Keshtkar H, Ashbaugh LL (2007) Size distribution of polycyclic aromatic hydrocarbon particulate emission factors from agricultural burning. Atmospheric Environment 41: 2729-2739.
[25] Phuleria HC, Sheesley RJ, Schauer JJ, Fine PM, Sioutas C (2007) Roadside measurements of size-segregated particulate organic compounds near gasoline and diesel-dominated freeways in Los Angeles, CA. Atmospheric Environment 41: 4653-4671.
[26] Kamens RM, Guo Z, Fulcher JN, Bell DA (1988) Influence of humidity, sunlight, and temperature on the daytime decay of polycyclic aromatic hydrocarbons on atmospheric soot particles. Environmental Science and Technology 22: 103-108.
[27] Lungren DA, Paulus HJ (1975) The mass distribution of large atmospheric particles. Journal of the Air Pollution Control Association 25: 1227-1231.
[28] Pierce RC, Katz M (1975) Dependency of polynuclear aromatic hydrocarbon content on size distribution of atmospheric aerosols. Environmental Science and Technology 9: 343–353.
[29] Venkataraman C, Lyons JM, Friendlander SK (1994) Size distributions of polycyclic aromatic hydrocarbons and elemental carbon. 1. Sampling, measurement methods, and source characterization. Environmental Science and Technology 28: 555-562.
[30] Venkataraman C, Friedlander SK (1994) Size distribution of polycyclic aromatic hydrocarbons and elemental carbon. 2. Ambient measurements and effects of atmospheric processes. Environmental Science and Technology 28: 563-572.
[31] Wiest F, Fiorentina HD (1975) Suggestions for a realistic definition of an air quality index relative to hydrocareonaceous matter associated with airborne particles. Atmospheric Environment 9: 951-954.
[32] Garivait H, Polprasert C, Yoshizumi K, Reutergardh LB (1999) Airborne polycyclic aromatic hydrocarbons (PAH) in Bangkok urban air I. Characterization and quantification. Polycyclic Aromatic Compounds 13: 313-327.
[33] Miguel AH, Kirchstetter TW, Harley RA (1998) On-road emissions of particulate polycyclic aromatic hydrocarbons and black carbon from gasoline and diesel vehicles. Environmental Science and Technology 32: 450–455.

[34] Zielinska B, Sagebiel J, McDonald JD, Whitney K, Lawson DR (2004) Emission rates and comparative chemical composition from selected in-use diesel and gasoline fueled vehicles; J. Air & Waste Manage. Assoc. 54(9):1138-50.

[35] Hoshiko T, Nakajima F, Prueksasit T, Yamamoto K (2012): 4. Health risk of exposure to vehicular emissions in wind-stagnant street canyons, In: "Ventilating cities -Air-flow criteria for healthy and comfortable urban living-" (Eds.: Kato S and Hiyama K), pp.59-95, Springer

IntechOpen

IntechOpen